An Enhanced Model-Based Algorithm for Early Internal Short Circuit Detection in Lithium-Ion Batteries

Yiqi Jia, Lorenzo Brancato, Marco Giglio and Francesco Cadini*

Politecnico di Milano, Department of Mechanical Engineering, via la Masa, 1, 20156, Milan, Italy

yiqi.jia@polimi.it
lorenzo.barncato@polimi.it
marco.giglio@polimi.it
**Corresponding author: francesco.cadini@polimi.it*

ABSTRACT

Electric vehicles (EVs) are becoming more popular due to concerns about fuel shortages and environmental pollution. Lithium-ion batteries are the preferred power source for EVs because they have high energy and power densities. Ensuring the efficient, safe, and reliable operation of these batteries has been a significant focus of research in recent decades. One major concern that can affect Li-ion battery performance is thermal runaway, which can cause dangerous battery fires. Internal short circuits (ISCs) are believed to be the root cause of thermal runaway incidents in batteries, making early detection of spontaneous ISCs a critical diagnostic task. This study presents a new and simple early ISC detection method for a Li-ion cell based on the augmentation of the state space of an Extended Kalman Filter (EKF) that includes voltage and surface temperature observations. The framework allows for an estimation of the cell's internal ISC state while remaining computationally efficient. The proposed approach is demonstrated in a simulated environment using dynamic stress tests that reflect a practical battery working cycle. The results demonstrate that the method can promptly detect ISC occurrences.

1. INTRODUCTION

In the recent years, LIBs have gained widespread popularity as portable energy sources in EVs among various types of batteries due to their significant advantages such as high energy density, high power density, and long lifetime (Goodenough & Kim, 2010). However, as rechargeable batteries, LIBs are subject to irreversible processes occurring during charging and discharging cycles, such as forming a solid-electrolyte interphase (SEI), severely impacting the electrochemistry of batteries. These processes typically result in continuous capacity fade, which eventually not only leads to battery failure but also a higher likelihood of severe safety problems, such as, catastrophic thermal runaway (TR) accidents. Therefore, a reliable battery management system (BMS) which can continuously monitor the health status of LIBs and diagnose any faults promptly to maintain the safe and reliable operation of appliances is necessary.

Internal short circuit (ISC) has been identified as the primary cause of thermal runaway (TR) in EVs during daily use. Although the exact mechanism of its formation has not been fully understood yet, based on its slow progression at an early stage, the early detection of ISC on BMS to prevent severer accidents is crucial and has therefore been the focus of many research efforts (G. Zhang et al., 2021) (Xiong et al., 2018) (Feng, Pan, et al., 2018). Nonetheless, it is a tough task for BMS to timely trace ISC progression by only observing the raw signals of sensors. Even though the thermal and electrical signals are affected by the presence of an ISC, these signals show a significant change only when the ISC has reached a middle or late stage, which prevents making early detection.

Different approaches have been studied in recent years to cope with this challenge (Asakura et al., 2010, 2012; Hermann & Kohn, 2013; Ikeuchi et al., 2014; Keates et al., 2010). Considering the application on BMS, a fast, simple integrated, and accurate diagnostic tool is developed in this work employing a model-based algorithms, specifically the extended Kalman filter (EKF) allowing to track in real-time the ISC evolution. To be specific, the voltage and temperature measurements obtained from BMS sensors can reveal hidden signals that are not immediately apparent. By analyzing these signals, it is possible to accurately determine the presence of Internal Short Circuit (ISC) in a LIB cell.

There are some research groups who worked on EKF-based ISC detection methods in the past years. In Yang's research, the soft ISC resistance value is estimated based on its relationship with the EKF algorithm's estimated SOC and calculated SOC (Yang et al., 2022). Similarly in the research of Hu et al. (Hu et al., 2020) the RLSVF algorithm has been applied to estimate the ISC current based on the SOC estimator. Feng et al. points out that the SOC difference and the heat negation power can be seen as ISC indicators, and results show that it can effectively detect the ISC (Feng, He, et al., 2018). However, the performance of these approaches

may be impacted by the low reliability of the open-loop state of charge (SOC) estimator. Overall, most of these proposed methods require post-processing based on the estimated value, are restricted by the working environment, cannot identify the level of soft ISC, or require an additional algorithm for the BMS to achieve the detection.

This paper presents a novel method that applies the EKF algorithm based on an equivalent circuit model (ECM)-ISC coupled with a thermal model to estimate the equivalent ISC resistance (RISC), relying on both electrical and thermal observations of the battery cell. From the value of the estimated RISC, the ISC not only can be identified, but also quantified. In the remainder of the paper, first the ECM-ISC-thermal plant model of battery cell is described and some ISC simulation results are shown in Section 2. Secondly, the EKF model-based detection method is explained and its detection performances are analyzed in Section 3. Finally, the conclusion are drawn in Section 4.

2. BATTERY CELL MODEL

2.1. ECM-ISC Model

Battery ECM has been widely applied for battery modelling because it is a good compromise between accuracy and complexity (Meng et al., 2019). This model consists of a variable voltage source, that is representative of the open-circuit behaviour of the cell, e.g., the so-called open-circuit voltage (OCV), which is usually approximated as a function of the cell SOC; a simple resistance element, to mimic the effect of voltage drops due to the linear polarization of the cell, and a theoretically infinite series of resistance-capacity networks to catch the slow voltage decays or relaxations related to diffusion processes happening within the cell; usually considering more than four RC subcircuits will not further improve the accuracy of the model (Plett, 2015). In this paper, we will consider two RC subcircuits for the cell modelling. As commonly done in the scientific literature (Feng et al., 2014; Kim et al., 2012; Zhao et al., 2015), by adding in parallel to the terminals of the ECM cell model an equivalent ISC resistance, the ISC effect on the cell measurements can be effectively mimicked. The graphical representation of the coupled ECM-ISC battery cell model is reported in Figure 1, where also the main parameters and variables of the model are outlined. Note that by assigning the value of the equivalent ISC resistance from 1000 Ω to 1 Ω , the levels of ISC can be simulated from no ISC, early ISC to moderate ISC (Lai et al., 2021).

The continuous-time equations governing the electrical dynamic of the ECM battery cell model are indicated hereafter:

$$z(t) = z_0 - \frac{1}{Q}\int_0^t i(t)dt \qquad (1)$$

$$\frac{di_{R_1}(t)}{dt} = -\frac{1}{R_1C_1}\, i_{R_1}(t) + \frac{1}{R_1C_1}\, i(t) \qquad (2)$$

$$\frac{di_{R_2}(t)}{dt} = -\frac{1}{R_2C_2}\, i_{R_2}(t) + \frac{1}{R_2C_2}\, i(t) \qquad (3)$$

$$v_t(t) = \mathrm{OCV}\big(z(t)\big) - Ri_R(t) - R_0 i(t) \qquad (4)$$

where z is the battery cell SOC, z_0 is the initial battery SOC, Q is the nominal capacity of the cell, R_1, R_2, C_1, C_2 and i_{R_1}, i_{R_2} are the resistances, capacities and the polarization current flowing in the two RC subcircuits, respectively; v_t is the battery cell terminal voltage.

We observe that when the value of R_{ISC} decreases, more current than the one required by the load is drawn by the battery cell, indeed, according to the Kirchhoff's current and voltage laws we have that $i(t) = i_t(t) + i_{ISC}(t)$ and $i_{ISC}(t) = v_t(t)/R_{ISC}$.

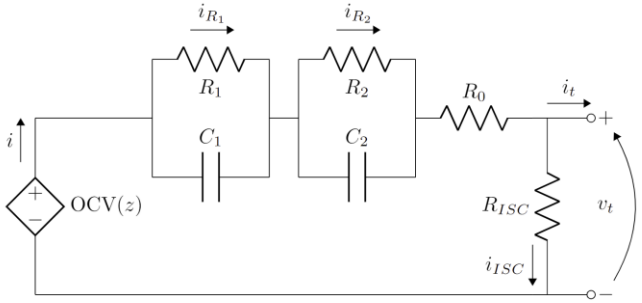

Figure 1. ECM battery cell model coupled with the ISC resistance in parallel.

2.2. Thermal Model

The thermal behavior of cell can be modelled employing a simplified version of the energy balance equation (EBE) proposed in the works of (Bernardi et al., 1985; Rao & Newman, 1997) similarly to what done in (Lai et al., 2021). The heat generated by the cell is mostly due to the losses occurring the resistance elements, and thus can be modelled according to:

$$Q_{in} = \int (R_0 i^2 + v_t^2/R_{ISC})dt\,. \qquad (4)$$

Assuming that the heat dissipates only through free convection with the surrounding air, the heat dissipated is simply given by:

$$Q_{out} = \int h(T_s - T_a)A\; dt\,. \qquad (5)$$

The EBE thus implies that the temperature evolution over time for the considered system is regulated by:

$$\dot{T}_s = \frac{\dot{Q}_{in} - \dot{Q}_{out}}{mc_m} \quad (6)$$

Combining Eq (5)-(7), the surface temperature evolution of battery cell can be expressed by:

$$\frac{dT_s(t)}{dt} = \\ = \frac{1}{mc_m}\left(R_0 i^2(t) + \frac{v_t(t)^2}{R_{ISC}} - h(T_s(t) - T_{amb})A\right), \quad (7)$$

where m is the mass of the cell, A is the outer surface area of the cell and c_m is the specific heat capacity of the cell; h is the air-free convection coefficient. This simple model can be employed if the temperature gradient within the battery cell can be assumed negligible, which is reasonable when considering small size battery cell.

2.3. Simulation results

In this section, the ECM-ISC-thermal model is simulated using MATLAB Simulink to show what is the effect of triggering an ISC on the outputs of the cell. In this work the ECM model of the ICR18650-22F battery cell, whose electrical characteristics (*SPECIFICATION OF PRODUCT (Tentative) for Lithium-Ion Rechargeable Cell Energy Business Division*, 2008) are reported in Table 1, is considered. Note that the size of this battery cell is relatively small.

Table 1. ICR18650-22F battery cell characteristics.

Name	Value
Nominal Capacity	2.2 Ah
Nominal Voltage	3.6 V
Weight	44.5 g
Size	Ø18.4 mm × 65 mm
Maximum Continuous Discharge Current	4.4A
Operating temperature range	Charge: 0 to 45°C Discharge: -20 to 60°C

For modelling this battery cell, the $\mathrm{OCV}(z)$ curve obtained at ambient temperature considering constant 1C discharging shown in Figure 2 (Safdari et al., 2022) is used. With concern to the thermal model parameter, the heat transfer coefficient h is set as 10 $\mathrm{W/m^2K}$, which is a typical value for air-free convection (Kosky et al., 2013); the heat capacity c_m is taken from a previous study on the LCO 18650 battery cell (X. Zhang et al., 2019), and is 896 J/kg/K; finally, the ambient temperature is assumed to be 298K.

The input load current used during the simulation is indicated in Figure 3. This is a 360 s Dynamic Stress Test (DST) current cycle, and is commonly employed when simulating the battery cell to obtain outputs that are representative of real life behaviours (Tian et al., 2014).

The ECM parameters adopted are shown in Table 2, and have been measured by a previous work (Tian et al., 2014) for the considered battery cell.

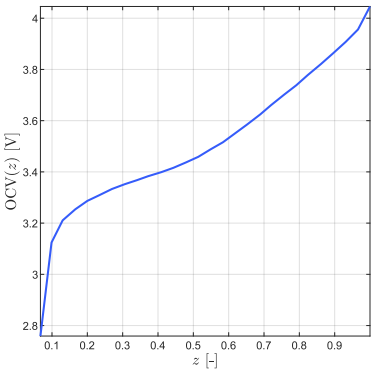

Figure 2. OCV-SOC characteristic for the ICR18650-22F battery cell when discharging at 1C.

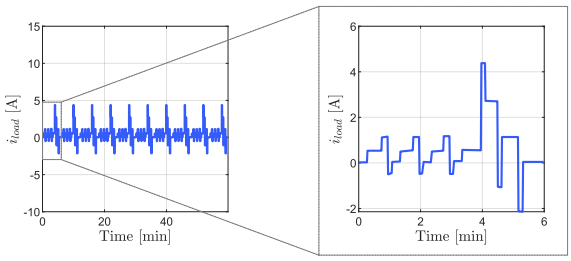

Figure 3. A periodic dynamic current profile for battery cell

Table 2. ECM parameters of ICR18650-22F battery cell.

Parameter	Value
R_0	0.00867 Ω
R_1	0.0124 Ω
R_2	0.0123 Ω
C_1	2239 F
C_2	41831 F

As also done in other works dealing with ISC detection methods, the ISC is suddenly triggered in the battery cell while it is discharging to assess the detection performance of the filter. The simulation is stopped when the cell is fully discharged or when the cell reaches a threshold temperature value of 50°C. Figure 4 illustrates the monitored terminal

voltage, surface temperature and SOC of the cell when different ISC intensities are triggered, i.e., absent ($R_{ISC} = 1000\Omega$), soft ($R_{ISC} = 100\Omega$) and moderate ($R_{ISC} = 10\ \Omega$).

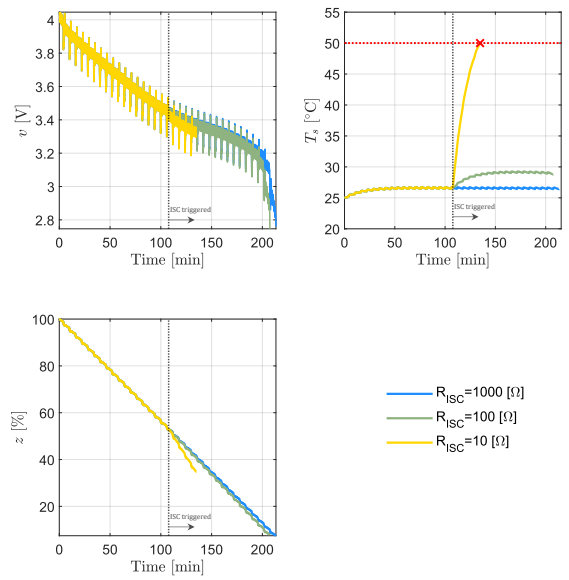

Figure 4. Battery behaviors simulated under various ISCs.

As Figure 4 demonstrates, it can be seen that the lower the ISC resistance, the faster the rise of temperature and the decrease of the terminal voltage. It is worth pointing out that even when the ISC is moderate (R_{ISC}=10 Ω), the temperature increase is quick.

3. ISC DETECTION METHOD AND DIAGNOSIS RESULTS

In this section it is shown how to use the EKF algorithm to jointly estimate the state and the equivalent ISC resistance of the ECM-ISC model. The estimated equivalent ISC resistance can then be exploited to perform ISC detection. In the following, the method used is briefly discussed and the results obtained are analyzed.

3.1. ISC detection method based on EKF

To implement EKF algorithm, Eq. (1)-(3) and Eq. (7) should be rewritten into a state-space formulation. In the ECM-ISC cell model there are four states, which can be gathered in the state vector $\mathbf{x}_k = \left[z_k, i_{R_1,k}, i_{R_2,k}, G_k\right]^T$, where $G = R_{ISC}^{-1}$ is the equivalent ISC conductance. Note that G is considered in place of R_{ISC} in the state vector to ease the calculation of the Jacobian matrices of the EKF algorithm; however, the correlation between G and R_{ISC} is straightforward. To allow the joint estimation of G, the input vector $\mathbf{u}_k = \left[i_{t,k}\ , v_k\right]^T$ is considered, like this the state-space realization of the stochastic ECM-ISC cell model indicated by Eq. (8) is obtained. In addition, the discrete-time noisy measurement equations are also specified by Eq. (9). These equations can be employed in a EKF to estimate the ECM-ISC cell model states. The estimation results are discussed in the next section.

$$\begin{aligned}\mathbf{x}_{k+1} &= \begin{bmatrix} z_{k+1} \\ i_{R_1,k+1} \\ i_{R_2,k+1} \\ G_{k+1} \end{bmatrix} \\ &= \begin{bmatrix} 1 & 0 & 0 & 0 \\ 0 & e^{-\frac{\Delta t}{R_1 C_1}} & 0 & 0 \\ 0 & 0 & e^{-\frac{\Delta t}{R_2 C_2}} & 0 \\ 0 & 0 & 0 & 1 \end{bmatrix} \begin{bmatrix} z_k \\ i_{R_1,k+1} \\ i_{R_2,k+1} \\ G_k \end{bmatrix} \\ &+ \begin{bmatrix} -\frac{\Delta t}{Q} & 0 \\ 1 - e^{-\frac{\Delta t}{R_1 C_1}} & 0 \\ 1 - e^{-\frac{\Delta t}{R_2 C_2}} & 0 \\ 0 & 1 \end{bmatrix} \begin{bmatrix} i_{t,k} + G_k v_{t,k} + w_{1,k} \\ w_{2,k} \end{bmatrix} \\ &= \mathrm{f}(\mathbf{x}_k, \mathbf{u}_k, \mathbf{w}_k), \end{aligned} \tag{8}$$

$$\begin{aligned}\mathbf{y}_{k+1} &= \begin{bmatrix} v_{t,k+1} \\ T_{s,k+1} \end{bmatrix} = \\ &\begin{bmatrix} \mathrm{OCV}(z_k) - R_1 i_{R_{1,k}} - R_2 i_{R_{2,k}} - R_0\left(i_{t,k} + G_k v_{t,k}\right) + n_{1,k} \\ T_{s,k} + \left[\frac{1}{mc_m}\left(R_0(i_{t,k} + G_k v_{t,k})^2 + G_k v_{t,k}^2 - h\left(T_{s,k} - T_a\right)\right)\right]\Delta t + n_{2,k} \end{bmatrix} \\ &= \mathrm{h}(\mathbf{y}_k, \mathbf{x}_k, \mathbf{u}_k, \mathbf{n}_k). \end{aligned} \tag{9}$$

3.2. ISC detection results

When simulating the online estimation of the ISC, first measurements of the EKF are generated by adding to the outputs of the ECM-ISC cell model (e.g., the voltage and the surface temperature) white noises, whose covariances are $\sigma_{n_1} = 10$ mV and $\sigma_{n_2} = 0.5$ K, respectively, to be more representative of real measured signals. The same covariance values have been used in (Bizeray et al., 2015) when estimating the battery cell internal state variables using EKF. The sampling time of the simulation is set to 100 ms, which is a reasonable value compared to commercial BMS applications (*Comparison Chart - Orion BMS*, n.d.).

In Figure 5 are shown the EKF estimation results when the ECM-ISC cell model is affected by a moderate ISC ($R_{ISC} = 10\Omega$). The results indicate that the EKF can promptly estimate the value of the equivalent ISC conductance with great accuracy, while also estimating the other internal states. This could be exploited in a BMS to perform early detection of the ISC state directly using the estimate of the equivalent ISC conductance, which can be also easily converted into the equivalent resistance.

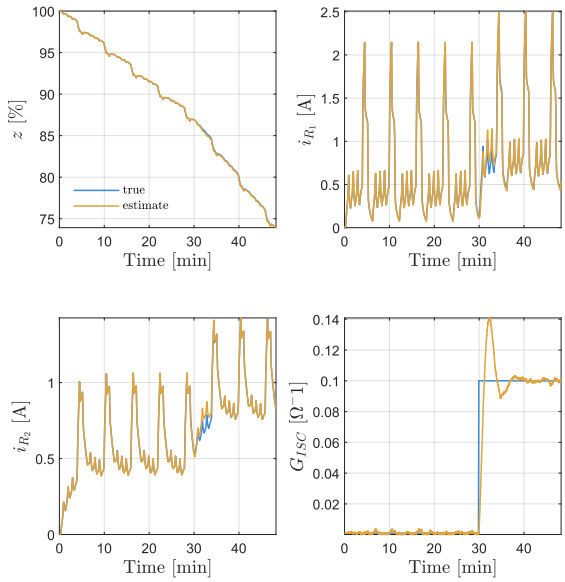

Figure 5. Detection results of the moderate ISC.

4. Conclusion

This paper proposes a novel method for early detecting internal short circuits (ISC) in Lithium-ion battery cells, that could be integrated into a BMS to improve safety. The method proposed is tested employing an equivalent circuit model (ECM) coupled with a thermal model to simulate the behavior of an ICR18650-22F battery cell with moderate and soft ISC under dynamic stress test (DST) working cycles. By measuring the surface temperature and terminal voltage of the battery cell, the proposed extended Kalman filter (EKF) model-based detection method can successfully detect the ISC and provide fast and accurate feedback of the equivalent ISC conductance G_{ISC} that can be used as the ISC state indicator for diagnostic purposes.

Nevertheless, there are some limitations in this work that need to be addressed in future research. A more realistic electrochemical model should be applied in place of the simple ECM model to better simulate real-world voltage measurements. Secondly, the proposed method employs a very simple thermal model that is only valid if small battery cells are considered. A more advanced 3D thermal model should be used instead when dealing with larger battery cells to correctly model the system behavior. Overall introducing a more realistic battery cell plant will introduce mismodelling errors and the performance of the proposed method should be tested.

Acknowledgement

The author Yiqi Jia would like to thank the China Scholarship Council for the financial support (CSC, No. 202108320086).

References

Asakura, J., Nakashima, T., Nakatsuji, T., & Fujikawa, M. (2010). *Battery internal short-circuit detecting device and method, battery pack, and electronic device system* (Patent No. US20100188054A1).

Asakura, J., Nakashima, T., Nakatsuji, T., & Fujikawa, M. (2012). *Battery internal short-circuit detection apparatus and method, and battery pack* (Patent No. US8334699B2).

Bernardi, D., Pawlikowski, E., & Newman, J. (1985). A General Energy Balance For Battery Systems. *Journal of the Electrochemical Society*, *132*(1), 5–12. https://doi.org/10.1149/1.2113792

Bizeray, A. M., Zhao, S., Duncan, S. R., & Howey, D. A. (2015). Lithium-ion battery thermal-electrochemical model-based state estimation using orthogonal collocation and a modified extended Kalman filter. *Journal of Power Sources*, *296*, 400–412. https://doi.org/10.1016/j.jpowsour.2015.07.019

Comparison Chart - Orion BMS. (n.d.). Https://Www.Orionbms.Com/Comparison/.

Fang, W., Ramadass, P., & Zhang, Z. (2014). Study of internal short in a Li-ion cell-II. Numerical investigation using a 3D electrochemical-thermal model. *Journal of Power Sources*, *248*, 1090–1098. https://doi.org/10.1016/j.jpowsour.2013.10.004

Feng, X., He, X., Lu, L., & Ouyang, M. (2018). Analysis on the Fault Features for Internal Short Circuit Detection Using an Electrochemical-Thermal Coupled Model. *Journal of The Electrochemical Society*, *165*(2), A155–A167. https://doi.org/10.1149/2.0501802jes

Feng, X., Pan, Y., He, X., Wang, L., & Ouyang, M. (2018). Detecting the internal short circuit in large-format lithium-ion battery using model-based fault-diagnosis algorithm. *Journal of Energy Storage*, *18*, 26–39. https://doi.org/10.1016/j.est.2018.04.020

Goodenough, J. B., & Kim, Y. (2010). Challenges for rechargeable Li batteries. In *Chemistry of Materials* (Vol. 22, Issue 3, pp. 587–603). https://doi.org/10.1021/cm901452z

Hermann, W. A., & Kohn, S. I. (2013). *Detection of over-current shorts in a battery pack using pattern recognition* (Patent No. US8618775B2).

Hu, J., Wei, Z., & He, H. (2020). Improved internal short circuit detection method for Lithium-Ion battery with self-diagnosis characteristic. *IECON Proceedings (Industrial Electronics Conference)*, *2020-October*, 3741–3746. https://doi.org/10.1109/IECON43393.2020.9254885

Ikeuchi, A., Majima, Y., Nakano, I., & KASAl, K. (2014). *Circuit and method for determining internal short-circuit, battery pack, and portable device* (Patent No. US20140184235A1).

Keates, A. W., Otani, N., Nguyen, D. J., Matsumura, N., & Li, P. T. (2010). *Short circuit detection for batteries* (Patent No. US7795843B2).

Kim, G.-H., Smith, K., Ireland, J., & Pesaran, A. (2012). Fail-safe design for large capacity lithium-ion battery systems. *Journal of Power Sources*, *210*, 243–253. https://doi.org/10.1016/j.jpowsour.2012.03.015

Kosky, P., Balmer, R., Keat, W., & Wise, G. (2013). Mechanical Engineering. In *Exploring Engineering* (pp. 259–281). Elsevier. https://doi.org/10.1016/B978-0-12-415891-7.00012-1

Lai, X., Jin, C., Yi, W., Han, X., Feng, X., Zheng, Y., & Ouyang, M. (2021). Mechanism, modeling, detection, and prevention of the internal short circuit in lithium-ion batteries: Recent advances and perspectives. In *Energy Storage Materials* (Vol. 35, pp. 470–499). Elsevier B.V. https://doi.org/10.1016/j.ensm.2020.11.026

Meng, J., Boukhnifer, M., & Diallo, D. (2019). *A Comparative Study of Open-Circuit-Voltage Estimation Algorithms for Lithium-Ion Batteries in Battery Management Systems; A Comparative Study of Open-Circuit-Voltage Estimation Algorithms for Lithium-Ion Batteries in Battery Management Systems*. https://doi.org/10.0/Linux-x86_64

Plett, G. L. (2015). *Battery Management Systems Volume I Battery Modeling*.

Rao, L., & Newman, J. (1997). Heat-generation rate and general energy balance for insertion battery systems. *Journal of the Electrochemical Society*, *144*(8), 2697–2704. https://doi.org/10.1149/1.1837884

Safdari, M., Ahmadi, R., & Sadeghzadeh, S. (2022). Numerical and experimental investigation on electric vehicles battery thermal management under New European Driving Cycle. *Applied Energy*, *315*. https://doi.org/10.1016/j.apenergy.2022.119026

SPECIFICATION OF PRODUCT (Tentative) for Lithium-ion Rechargeable Cell Energy Business Division. (2008).

Tian, Y., Xia, B., Wang, M., Sun, W., & Xu, Z. (2014). Comparison study on two model-based adaptive algorithms for SOC estimation of lithium-ion batteries in electric vehicles. *Energies*, *7*(12), 8446–8464. https://doi.org/10.3390/en7128446

Xiong, R., Li, L., & Tian, J. (2018). Towards a smarter battery management system: A critical review on battery state of health monitoring methods. In *Journal of Power Sources* (Vol. 405, pp. 18–29). Elsevier B.V. https://doi.org/10.1016/j.jpowsour.2018.10.019

Yang, R., Xiong, R., & Shen, W. (2022). On-board diagnosis of soft short circuit fault in lithium-ion battery packs for electric vehicles using an extended Kalman filter. *CSEE Journal of Power and Energy Systems*, *8*(1), 258–270. https://doi.org/10.17775/CSEEJPES.2020.03260

Zhang, G., Wei, X., Tang, X., Zhu, J., Chen, S., & Dai, H. (2021). Internal short circuit mechanisms, experimental approaches and detection methods of lithium-ion batteries for electric vehicles: A review. In *Renewable and Sustainable Energy Reviews* (Vol. 141). Elsevier Ltd. https://doi.org/10.1016/j.rser.2021.110790

Zhang, X., Klein, R., Subbaraman, A., Chumakov, S., Li, X., Christensen, J., Linder, C., & Kim, S. U. (2019). Evaluation of convective heat transfer coefficient and specific heat capacity of a lithium-ion battery using infrared camera and lumped capacitance method. *Journal of Power Sources*, *412*, 552–558. https://doi.org/10.1016/j.jpowsour.2018.11.064

Zhao, W., Luo, G., & Wang, C.-Y. (2015). Modeling nail penetration process in large-format li-ion cells. *Journal of the Electrochemical Society*, *162*(1), A207–A217. https://doi.org/10.1149/2.1071501jes

Yiqi Jia

Lorenzo Brancato

Marco Giglio

Francesco Cadini